

20. M. Pagano *et al.*, *Science* **269**, 682 (1995).
21. Abbreviations for the amino acid residues are as follows: C, Cys; D, Asp; E, Glu; F, Phe; G, Gly; H, His; K, Lys; L, Leu; N, Asn; P, Pro; Q, Gln; R, Arg; T, Thr; V, Val; W, Trp; and Y, Tyr.
22. V. Dulić, E. Lees, S. I. Reed, *Science* **257**, 1958 (1992).
23. HeLa cells were grown to 3×10^5 cells/ml and arrested with thymidine (2 mM) or lovastatin (40 μ M) for 24 hours. Cells (5×10^7) were collected by centrifugation, washed in phosphate-buffered saline (PBS), and resuspended in 50 ml of Dulbecco's modified Eagle's medium (DMEM) without methionine and cysteine (ICN) and with thymidine, lovastatin, or no drug. Tran³⁵S label (1 mCi; ICN) was added, and the cells were pulse-labeled for 60 min. After the pulse, methionine and cysteine were added to final concentrations of 100 or 150 mg/liter. At the time points shown, samples of cells were collected by centrifugation, washed in PBS, and lysed in RIPA buffer [in PBS: 1% NP-40, 0.5% sodium deoxycholate, 0.1% SDS, phenylmethylsulfonyl fluoride (PMSF; 0.1 mg/ml), aprotinin (30 μ l/ml; Sigma), and 0.1 mM sodium orthovanadate]. Protein concentrations were determined by absorbance at 280 nm, and equal amounts of protein extracts were used for p27 immunoprecipitation with an antibody to p27, generated against amino acids 181 to 198 of p27 [p27-C19 (Santa Cruz Biotechnology, Santa Cruz, CA), suitable for immunodepletion of the nondepleted protein]. Immune complexes were collected on protein A-Sepharose beads and washed five times in RIPA buffer and once in RIPA buffer containing methionine and cysteine (each at 1 mg/ml). The immunoprecipitates were separated by SDS-PAGE, treated with Amplify (Amersham), and used for autoradiography. For pulse-labeling experiments, increased amounts of cells (3.5×10^7 cells/10 ml) and radioactivity (1.5 mCi/10 ml) were used, and cells were starved for 60 min in medium lacking methionine and cysteine before labeling.
24. HeLa cells were grown in suspension culture at densities of 2×10^5 to 6×10^5 cells/ml in DMEM supplemented with newborn calf serum (10%). Asynchronous growing cells were arrested in G₁ by treatment with 66 μ M lovastatin for 33 hours as described [K. Keyomarsi, L. Sandoval, V. Band, A. B. Pardee, *Cancer Res.* **51**, 3602 (1991)]. For fluorescence-activated cell sorting (FACS) analyses, 5-ml samples were labeled for 15 min with bromodeoxyuridine (BrdU; 30 μ g/ml). The distribution of the cells in the cell cycle was determined with monoclonal antibodies to BrdU (anti-BrdU) and staining with propidium iodide (Becton Dickinson) according to the manufacturer's directions. Proteins and RNA were isolated with the Tri Reagent system (Molecular Research Center). Immunoblots of cyclins, Cdk's, and p27 were performed with polyclonal (anti-p27 and anti-cyclin A) or monoclonal antibodies (anti-cyclin E and anti-PSTAIRE) as described (22). Antibodies to p27 were generated against a peptide sequence (CRNLFGPVDHEEL-TRDLE) (21) from the p27 protein, and antibodies affinity-purified against the immunogenic peptide were used. Polyclonal antibodies to p21 were generated with the full-length protein as antigen. RNA was separated through 1% agarose gels, transferred to Nytran plus membrane (Schleicher & Schuell), and hybridized at 65°C in 1 M NaCl, 10% dextran sulfate, 1% SDS, and salmon testis DNA (100 μ g/ml).
25. Asynchronously growing human newborn foreskin fibroblasts (HS68) cells were diluted 1:3, seeded in DMEM supplemented with fetal bovine serum (FBS; 10%) at 20% confluency, and grown into contact inhibition. For FACS analyses, cells on one plate were labeled for 30 min with BrdU (30 μ g/ml).
26. HL60 human promyelocytic leukemia cells were grown in RPMI 1640 medium supplemented with 20% heat-inactivated FBS. Differentiation to monocytes was induced by adding 1 α , 25-dihydroxy vitamin D₃ (Biomol; 10^{-7} M final concentration) and indomethacin (Biomol; 18.75 μ g/ml final concentration).
27. HeLa cells were grown in suspension culture at densities of 2×10^5 to 6×10^5 cells/ml in DMEM supplemented with newborn calf serum (10%). Cells were synchronized by a thymidine and nocodazole block release protocol with 2 mM thymidine for 19 hours, released for 3 hours, and treated with nocodazole (75 ng/ml) for 12 hours. Samples of the synchronized cells were harvested every hour after release from the nocodazole block, and the percentage of cells in different phases of the cell cycle was determined by FACS analysis as described (13).
28. HS68 human diploid fibroblasts were grown to confluency and incubated for three additional days in DMEM growth medium, supplemented with 10% heat-inactivated FBS. Cells were trypsinized and seeded in a dilution of 1:5. Samples were taken at 3-hour intervals after release from the contact inhibition. For FACS analyses, samples were labeled for 15 min with BrdU (30 μ g/ml).
29. HeLa cells were incubated in 2 mM thymidine for 22 hours. For each time point, a 10-ml cell suspension was incubated in DMEM without methionine and cysteine (ICN) at 6×10^6 cells/ml for 30 min. After addition of 1.8 mCi Tran³⁵S label (ICN) per sample (10 ml), cells were labeled for 30 min and incubated for 0, 15, 30, 60, or 120 min in the presence of methionine (100 mg/liter) and cysteine (150 mg/liter). Cells were collected by centrifugation, washed in PBS, and lysed in RIPA buffer [in PBS: 1% NP-40, 0.5% sodium deoxycholate, 0.1% SDS, PMSF (0.1 mg/ml), aprotinin (30 μ l/ml; Sigma), and 0.1 mM sodium orthovanadate]. Protein concentrations were determined by absorbance at 280 nm, and samples were adjusted for equal protein amounts. Proteins were denatured by boiling at 100°C for 5 min. p27 was precipitated with a polyclonal antibody to p27 (C19) (23). Immune complexes were collected on protein A-Sepharose beads and washed seven times in RIPA buffer and once in RIPA buffer containing methionine and cysteine (each at 1 mg/ml). The immunoprecipitates were separated by SDS-PAGE and used for autoradiography.
30. HS68 human diploid fibroblasts were grown to contact inhibition and used after 6 days of density-mediated growth arrest. Asynchronous cells were grown to <30% confluency on plates. Labeling was done as described (23). Labeled cells were washed with PBS, scraped in RIPA buffer, extracts were normalized for equal counts per minute (cpm), and p27 immunoprecipitated as described (23).
31. HS68 human diploid fibroblasts were labeled 4 days after density-mediated growth arrest. Asynchronous cells were grown to <30% confluency on plates. Pulse-chase labeling was done as described (23). The labeled cells were washed with PBS, trypsinized, and washed several times with ice-cold PBS. Cells were lysed in RIPA buffer, the extracts were normalized for equal cpm, and p27 immunoprecipitated as described (23).
32. Contact-inhibited HS68 human diploid fibroblasts were labeled 3 days after density-mediated growth arrest cells. Asynchronous cells were grown to 45% confluency on plates. Cells were labeled for 30 min with 350 μ Ci of Tran³⁵S label in 10 ml of DMEM without methionine and cysteine (ICN) (per plate). Cells were washed in ice-cold PBS and scraped in PBS containing 1% NP-40 and PMSF (0.1 mg/ml), aprotinin (30 μ l/ml; Sigma), and 0.1 mM sodium orthovanadate. The extracts were normalized for equal cpm and boiled for 10 min. The heat-stable supernatant containing almost all p27 protein was adjusted to 0.5% sodium deoxycholate and 0.1% SDS. The p27 protein was precipitated with affinity-purified antibody generated against a p27 peptide sequence (24). The second antibody cross-reacts with the p21 protein. Immunoprecipitates were washed once in RIPA and three times in PBS containing 1% NP-40, separated by SDS-PAGE, and analyzed by autoradiography.
33. We thank A. W. Alberts for lovastatin; T. Hunter, R. Poon, and H. Toyoshima for communicating results before publication; and S. Haase, F. Melchior, B. Niculescu, and K. Sato for critical reading of the manuscript. Supported by fellowships from the Leukemia Society of America (to L.H.) and by U.S. Public Health Service grant GM46006 and U.S. Army grant DAMD17-94-J4208 (to S.I.R.).

21 August 1995; accepted 30 January 1996

Altered Sensory Processing in the Somatosensory Cortex of the Mouse Mutant *Barrelless*

E. Welker,* M. Armstrong-James, G. Bronchti, W. Ourednik, F. Gheorghita-Baechler, R. Dubois, D. L. Guernsey, H. Van der Loos, P. E. Neumann

Mice homozygous for the *barrelless* (*brl*) mutation, mapped here to chromosome 11, lack barrel-shaped arrays of cell clusters termed "barrels" in the primary somatosensory cortex. Deoxyglucose uptake demonstrated that the topology of the cortical whisker representation is nevertheless preserved. Anterograde tracers revealed a lack of spatial segregation of thalamic afferents into individual barrel territories, and single-cell recordings demonstrated a lack of temporal discrimination of center from surround information. Thus, structural segregation of thalamic inputs is not essential to generate topological order in the somatosensory cortex, but it is required for discrete spatiotemporal relay of sensory information to the cortex.

Segregation in the processing of peripheral information is a common principle in the organization of sensory cortical areas. This principle was first demonstrated in the primary visual cortex of cats and monkeys, in which segregation of thalamocortical axons forms the anatomic basis for ocular dominance columns (1). In rodents, the pattern of mystacial whisker follicles is replicated in

layer IV of the primary somatosensory cortex (SI) by an array of cell clusters named "barrels" (2). Each barrel is activated by an individual whisker, the "center" whisker, through fast thalamocortical relay, but it also integrates information from neighboring whiskers (3) through slower intracortical circuitry (4). The one-to-one correspondence between whisker follicles and their

cortical representation results from the segregation of thalamocortical axons into barrel domains (5, 6). These axons initiate the parcellation of SI during development (7), and their geometry is modified after neonatal follicle injury (8). A spontaneous mutation in our mouse colony generated animals in which the parcellation of SI into barrels does not occur. This mutation has allowed us to investigate the role of barrels in particular, and parcellation of the cerebral cortex in general, in sensory processing.

Barrelless mice were discovered in a line bred for a normal pattern of mystacial vibrissae (9) and now form a true-breeding line. The barrelless phenotype is an autosomal recessive trait. In crosses with C57BL/6J inbred mice, 15 of 32 backcross offspring and 6 of 46 intercross offspring were barrelless. On the basis of simple sequence length polymorphisms (10), the *barrelless* (*brl*) locus was mapped to the proximal segment of chromosome 11 because no recombination with the microsatellite D11Mit226 was detected in these offspring. Barrelless mice show no other sign of neurological disorganization.

The cytoarchitectural contours of individual barrels typical of normal mice (Fig. 1, A and C) cannot be detected in layer IV of SI of barrelless mice (Fig. 1, B and D). However, the distribution of layer IV cells does not always appear uniform, and the faint representation of rows of whisker follicles can sometimes be discerned. The patterning varies among animals, and that shown in Fig. 1B is one of the clearest examples observed. In the brainstem trigeminal complex of mutant mice (Fig. 1, H and J), whisker-related patterns are visible as in normal animals (Fig. 1, G and I) [see (11)]. The whisker-related parcellation of the ventrobasal nucleus of the thalamus into "barreloids" (12) is less clear in the mutant (Fig. 1F) than in normal (Fig. 1E) mice. In barrelless mice, the patterns in brainstem and thalamus appear at the same times as those in normal mice (13). Except for the absence of barrels in the mutant mice, the somatosensory cortex of these animals shows no cytoarchitectonic abnor-

malities at any postnatal age. This aspect of the barrelless phenotype is similar to that in monoamine oxidase A-deficient mice (14).

Arborizations of thalamocortical axons (TCAs) were mostly confined to barrels in layer IV of SI in normal mice (Fig. 2A), with a less dense projection to upper layer VI (Fig. 2C) (15). In barrelless mice, TCAs also terminated in layers IV and VI but were continuously distributed in layer IV, rather than being confined to barrel-like structures (Fig. 2, B and D). The labeling

did not show a row-like pattern in any of the barrelless mouse brains examined in a tangential plane. In normal animals, individual TCA arbors were restricted to one barrel (Fig. 2E), confirming earlier studies (5). In barrelless mice, these arbors extended within layer IV over distances that would incorporate a tangential area of up to 10 normal barrels (Fig. 2F). Thus, substantial overlap of TCA arbors appropriate to adjacent whiskers must occur in barrelless animals.

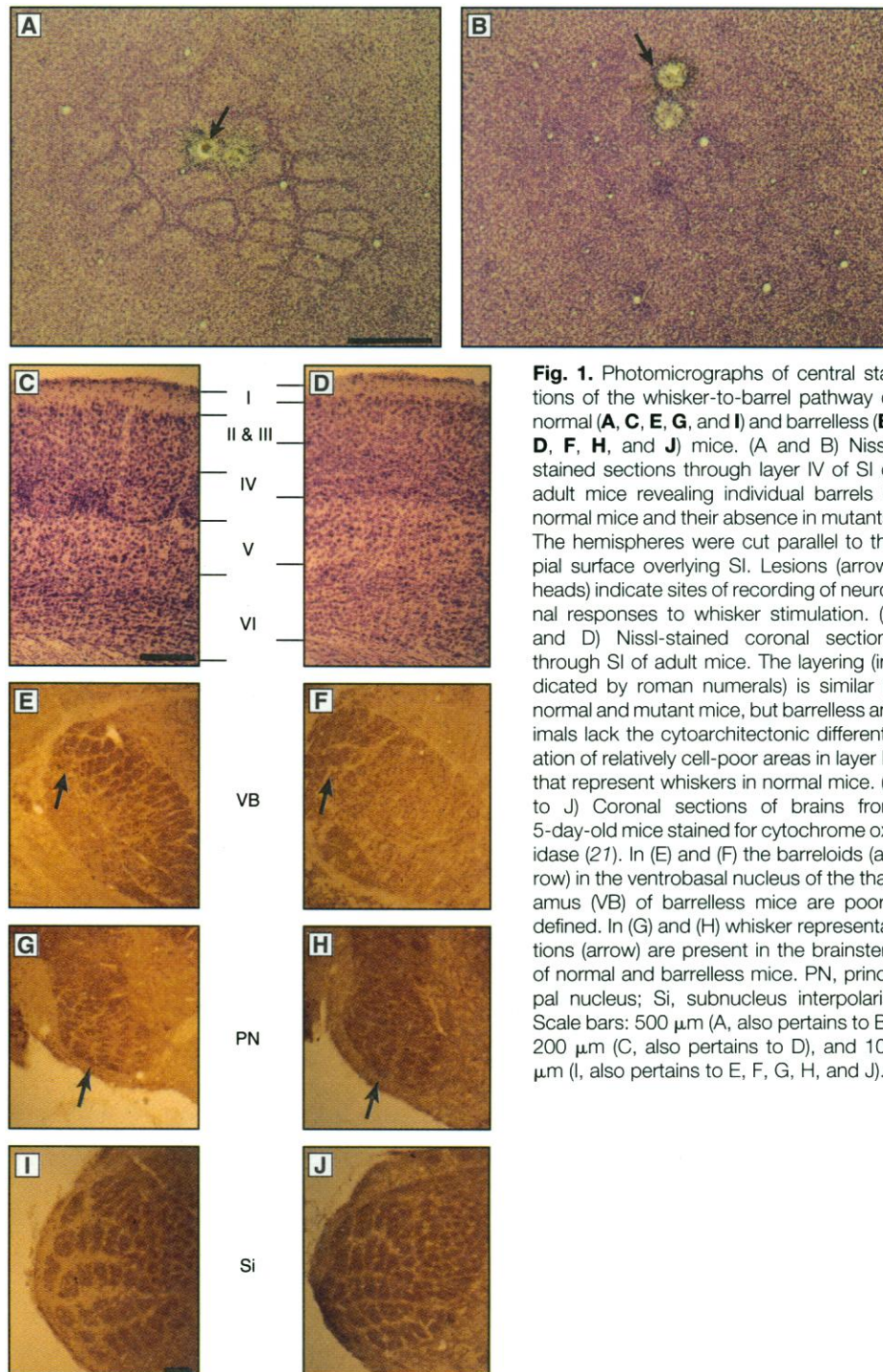


Fig. 1. Photomicrographs of central stations of the whisker-to-barrel pathway of normal (A, C, E, G, and I) and barrelless (B, D, F, H, and J) mice. (A and B) Nissl-stained sections through layer IV of SI of adult mice revealing individual barrels in normal mice and their absence in mutants. The hemispheres were cut parallel to the pial surface overlying SI. Lesions (arrowheads) indicate sites of recording of neuronal responses to whisker stimulation. (C and D) Nissl-stained coronal sections through SI of adult mice. The layering (indicated by roman numerals) is similar in normal and mutant mice, but barrelless animals lack the cytoarchitectonic differentiation of relatively cell-poor areas in layer IV that represent whiskers in normal mice. (E to J) Coronal sections of brains from 5-day-old mice stained for cytochrome oxidase (27). In (E) and (F) the barreloids (arrow) in the ventrobasal nucleus of the thalamus (VB) of barrelless mice are poorly defined. In (G) and (H) whisker representations (arrow) are present in the brainstem of normal and barrelless mice. PN, principal nucleus; Si, subnucleus interpo-laris. Scale bars: 500 μ m (A, also pertains to B), 200 μ m (C, also pertains to D), and 100 μ m (I, also pertains to E, F, G, H, and J).

E. Welker, G. Bronchti, F. Gheorghita-Baechler, R. Dubois, H. Van der Loos, Institute of Anatomy, University of Lausanne, Rue du Bugnon 9, 1005 Lausanne, Switzerland.

M. Armstrong-James, Department of Physiology, Queen Mary and Westfield College, London E1 4NS, United Kingdom.

W. Ourednik, Department of Anatomy and Neurobiology, Dalhousie University, Halifax, Nova Scotia, Canada B3H 4H7.

D. L. Guernsey, Division of Molecular Pathology and Molecular Genetics, Department of Pathology, Dalhousie University, Halifax, Nova Scotia, Canada B3H 4H7.

P. E. Neumann, Department of Anatomy and Neurobiology, and Division of Molecular Pathology and Molecular Genetics, Department of Pathology, Dalhousie University, Halifax, Nova Scotia, Canada, B3H 4H7.

*To whom correspondence should be addressed.

Deoxyglucose (DG) uptake measurements showed that the normal topology of the whisker representation was preserved in barrelless mice (Fig. 3). Behavioral activation of whiskers of rows B and D produced two separated uptake zones in layer IV, leaving a relatively DG-free area representing the intermediate C row, in both barrelless and normal animals (16). The distance between the centers of the two DG spots was similar in the two lines of mice: $677 \pm 28 \mu\text{m}$ (mean \pm SD, $n = 6$) in normal mice and $685 \pm 55 \mu\text{m}$ ($n = 6$) in barrelless animals. Moreover, no significant difference was apparent between the two lines in

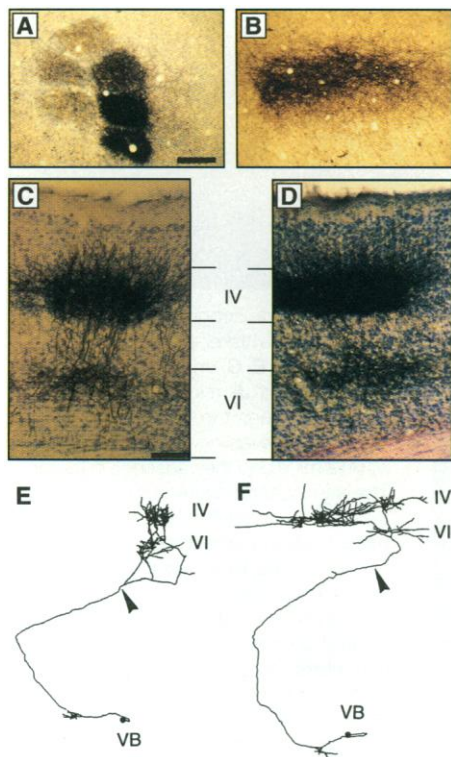


Fig. 2. Thalamocortical projections from the ventrobasal nucleus of the thalamus (VB) in normal (A, C, and E) and barrelless (B, D, and F) mice. (A and B) Tangential sections through layer IV of SI of normal mice reveal labeling (dextran) that is confined to the inside of barrels (relatively free of label). In barrelless mice, labeling forms a continuous zone. Although intracortical collaterals of retrogradely labeled neurons may have contributed to the labeling, the photomicrographs illustrate the lack of tangential segregation of TCAs in barrelless mice. (C and D) Coronal sections through SI reveal labeling (dextran) in layer IV and in the upper part of layer VI in both strains. (E and F) Individual TCAs (biocytin-labeled) were reconstructed with a computer microscope and the NeuroLucida program (MicroBrightfield, Colchester, Vermont, USA). Arrowheads indicate the site where the axon enters SI. The axon of the normal mouse terminates in a confined area of SI, whereas in barrelless animals it terminates in a large area. Scale bars: 200 μm (A, also pertains to B), 100 μm (C, also pertains to D), and 500 μm (E, also pertains to F).

the areal extent of the zones of stimulus-dependent DG uptake, as determined at levels of 25 and 50% above background.

Exploratory penetrations of SI during physiological recording sessions also indicated the same topological order for whisker representation in barrelless and normal mice. We analyzed the magnitude and latency of single-unit responses to activation of center and surround whiskers (Fig. 4) (17). In normal animals ($n = 7$; 33 units), the response to the fastest surround whisker was one-third the magnitude of that to the center whisker, with a latency that was 5 to 25 ms greater than that for the center whisker. In barrelless mice ($n = 10$; 44 units), response magnitudes to surround whiskers were larger than those in normal mice, about one-half those to the center whisker, and notably, these responses did not differ significantly in latency from those to the center whisker. This lack of temporal separation and the greater surround response in barrelless mice correlate well with the extensive spatial overlap of TCA arbors: A layer IV neuron in mutant animals receives converging thalamic input from several whisker follicles. These profound functional differences in receptive field organization between the two lines are not reflected in DG uptake, which appears to represent the response to the center whiskers only.

Fig. 3. Cortical representations of the three caudal-most whiskers of rows B and D in normal and barrelless mice as revealed by DG uptake. The extent of DG uptake is represented by color (according to the indicated scales). In normal mice, stimulus-dependent DG uptake was confined to barrels (reconstructed from the counterstained sections) corresponding to the stimulated whiskers. A similar pattern was apparent in barrelless mice. The plots represent the mean density of DG label (in nanocuries per gram of brain tissue) measured in the zone delineated by the small line segments placed near the border of the pseudocolor images. The distance between centers of representation of rows B and D was measured (horizontal arrows).

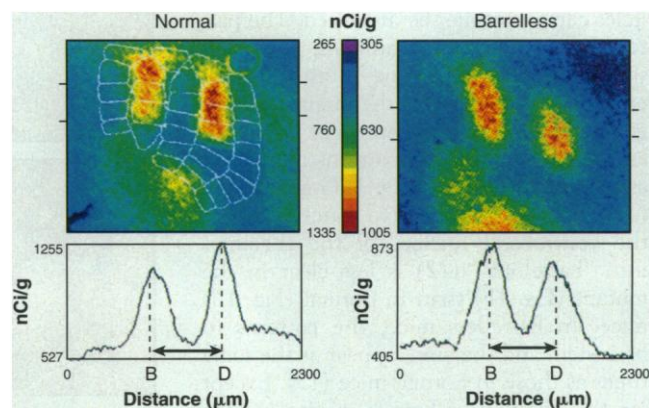
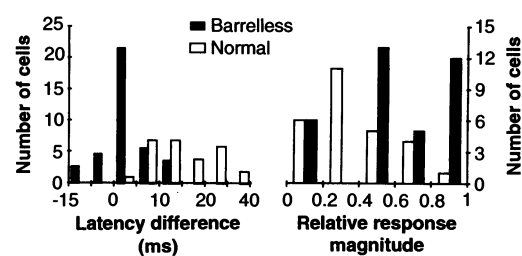


Fig. 4. Response characteristics of layer IV neurons in normal barrelless mice. (Left) Distribution of differences in response latencies to the center and surround whiskers. In normal mice, the median latency difference was 13.5 ms [interquartile range (IQR), 9.0 to 21.0 ms], whereas in barrelless mice it was 2.5 ms (IQR, 0.9 to 4.6 ms; $P < 0.0001$, Mann-Whitney test). (Right) Distributions of relative response magnitudes of surround whiskers to center whiskers. In normal mice, the response ratio (surround/center) was 0.33 (IQR, 0.21 to 0.57), whereas in barrelless mice it was 0.56 (IQR, 0.43 to 0.83; $P < 0.003$, Mann-Whitney test).



Homozygosity for *barrelless* is associated with a partial failure of patterning of the whisker-to-barrel pathway. The normal formation of whisker representations in the brainstem of barrelless mice suggests that the mutation may affect segregation of axonal arbors at the level of VB (afferents from the trigeminal brainstem) and somatosensory cortex (TCAs), or that it might disturb maturation of VB, resulting in incomplete formation of barreloids and aberrant TCA arborization. The row-like organization apparent in the distribution of cortical neurons of some mice may reflect an early step in the development of barrel cortex but occurs to a variable extent in barrelless mice. Cortical lamination as well as overall size and topological organization of the cortical whisker representation remains unaffected in barrelless mice, providing evidence that different aspects of the patterning of the cerebral cortex are at least partially independent (18).

We conclude that the failure of TCA arbors to segregate in barrelless mice does not affect the topological organization of the somatosensory cortex. The overlap of TCAs in this mutant is greater than suggested by the topology demonstrated by DG uptake. A comparable situation was observed in SI of monkeys, in which TCA arbors also span a greater cortical area than

the functionally determined topological map (19). We also conclude that the functional operation of the cerebral cortex depends on the pattern of thalamocortical connectivity. Segregation of TCAs in sensory cortex promotes independence of processing inputs that characterize neighboring, but nonadjacent, groups of sensory receptors such as whisker follicles. Overlap of TCAs in barreless mice generates receptive fields of cortical neurons that are more appropriate to a continuous and less discriminate representation of the tactile periphery. This overlap excludes the possibility that single-whisker information can be processed separately within a discrete group of cortical neurons before further intracortical relay. Most theories on sensory discrimination and map modification by sensory experience depend on precise spatiotemporal ordering of sensory inputs (20). The defective temporal differentiation and impaired spatial separation of sensory inputs uncovered here within the somatosensory cortex of barreless mice provide a model for testing such hypotheses.

acetate) was iontophoretically injected (150 nA of positive current, 1 s on and 1 s off for 10 to 15 min) through a pipette with a diameter of 1 to 3 μ m. After a survival period of 1 week (dextran) or 24 hours (biocytin), mice were deeply anesthetized and processed as described [M. J. Dolleman-Van der Weel, F. G. Wouterlood, M. P. Witter, *J. Neurosci. Methods* **51**, 9 (1994)]. The injection site was verified histologically.

16. Mystacial whiskers are distributed in five horizontal rows (named A through E). For the DG uptake experiments, the caudalmost whiskers of rows A, C, and E were clipped on the left side. Animals were injected intraperitoneally with 2-[1-¹⁴C]deoxy-D-glucose (16.5 μ Ci per 100 g of body mass) and placed in an object-filled cage for 45 min, after which they were anesthetized and their brains processed for autoradiography [E. Welker, S. B. Rao, J. Dörfel, P. Melzer, H. Van der Loos, *J. Neurosci.* **12**, 153 (1992)].
17. Recordings were made from mice under urethane anesthesia (2 mg per gram of body mass, administered by intraperitoneal injections of a 10% solution in distilled water). Units were situated 350 to 480 μ m below the pial surface. The center whisker was defined as that giving the largest response magnitude.

Data for the surround whisker refer to the one with the shortest latency. Response magnitudes were measured by the mean number of spikes generated per 50 deflections [E. Welker, M. Armstrong-James, H. Van der Loos, R. Kraftsik, *Eur. J. Neurosci.* **5**, 691 (1993)].

18. M. Cohen-Tannoudji, C. Eabinet, M. Wassef, *Nature* **368**, 460 (1994).
19. E. Garraghty and M. Sur, *J. Comp. Neurol.* **294**, 583 (1990).
20. C. Von der Malsburg, in *The Neural and Molecular Bases of Learning*, J.-P. Changeux and M. Konishi, Eds. (Wiley, New York, 1987), pp. 411–431.
21. M. Wong-Riley, *Brain Res.* **171**, 11 (1979).
22. Our dear collaborator Hendrik Van der Loos died in October 1993. We thank N. Trapp and G. Skabarodonis for technical assistance and S. Catsicas, P. G. H. Clarke, A. Fine, J.-P. Hornung, G. M. Innocenti, and J. H. Kaas for comments on the manuscript. Supported by the Swiss National Science Foundation (grant 31-39184), the Wellcome Trust (M.A.-J.), and the Medical Research Council of Canada (grant MT-12941).

24 July 1995; accepted 11 January 1996

A Neural Tetraspanin, Encoded by *late bloomer*, That Facilitates Synapse Formation

Casey C. Kopczynski, Graeme W. Davis, Corey S. Goodman*

Upon contacting its postsynaptic target, a neuronal growth cone transforms into a pre-synaptic terminal. A membrane component on the growth cone that facilitates synapse formation was identified by means of a complementary DNA-based screen followed by genetic analysis. The *late bloomer (lbl)* gene in *Drosophila* encodes a member of the tetraspanin family of cell surface proteins. LBL protein is transiently expressed on motor axons, growth cones, and terminal arbors. In *lbl* mutant embryos, the growth cone of the RP3 motoneuron contacts its target muscles, but synapse formation is delayed and neighboring motoneurons display an increase in ectopic sprouting.

As neuronal growth cones encounter a variety of guidance cues, they steer toward attractive signals and away from repulsive ones (1). Ultimately, they reach their targets, shut down their motility machinery, retract their filopodia, and transform into presynaptic terminals. In *Drosophila*, genetic analysis can be used to dissect the molecular machinery of synapse formation at the embryonic neuromuscular junction (2). In each abdominal hemisegment, some 40 motoneurons make specific synaptic connections with 30 identified muscle fibers. For example, the RP3 motoneuron forms synapses on muscles 7 and 6 (3).

We designed a complementary DNA (cDNA)-based reverse genetic approach to identify molecules involved in growth cone guidance, target recognition, and synapse formation (4). In an effort to bias our search toward molecules involved in cell-cell interactions, we purified mRNA from rough endoplasmic reticulum-bound polysomes

and used it to prepare a cDNA library that was enriched and then normalized for clones encoding membrane and secreted proteins. We initially screened 850 clones by large-scale whole mount in situ hybridization to identify clones that hybridize to subsets of neurons or their targets during development. Here, we describe the *lbl* gene that functions to facilitate the establishment of neuromuscular synapses.

An *lbl* cDNA, p3B6, was identified as a clone that hybridizes to a specific subset of neurons in the embryonic central nervous system (CNS). All motoneurons that can be uniquely identified express *lbl*, including aCC, RP1 through RP5, the three U's, and the VUMs; for example, aCC (a motoneuron) expresses *lbl*, whereas its sibling, pCC (an interneuron), does not (Fig. 1A). A lateral cluster of neurons that is coincident with the major cluster of other motoneurons also expresses *lbl* (Fig. 1B), which further suggests that *lbl* is expressed specifically by motoneurons (5). Some peripheral sensory neurons also express *lbl*, but transiently and in much smaller amounts (6).

The nearly exclusive restriction of *lbl* expression by motoneurons was confirmed

REFERENCES AND NOTES

1. D. H. Hubel and T. N. Wiesel, *J. Comp. Neurol.* **146**, 421 (1972); S. Levay, D. H. Hubel, T. N. Wiesel, *ibid.* **159**, 559 (1975); S. Levay, M. P. Stryker, C. J. Shatz, *ibid.* **179**, 223 (1978); M. P. Stryker and W. A. Harris, *J. Neurosci.* **6**, 2117 (1986).
2. T. A. Woolsey and H. Van der Loos, *Brain Res.* **17**, 205 (1970); T. A. Woolsey, C. Welker, R. H. Schwartz, *J. Comp. Neurol.* **164**, 79 (1975).
3. D. J. Simons, *J. Neurophysiol.* **54**, 615 (1985); M. Armstrong-James and K. Fox, *J. Comp. Neurol.* **263**, 265 (1987).
4. M. Armstrong-James, C. A. Callahan, M. A. Friedman, *J. Comp. Neurol.* **303**, 193 (1991); K. Fox, *J. Neurosci.* **14**, 7665 (1994).
5. R. Lorente de Nó, *Trab. Lab. Invest. Biol. Univ. Madrid* **20**, 41 (1922); K. F. Jensen and H. P. Killackey, *J. Neurosci.* **7**, 3529 (1987).
6. S. L. Senft and T. A. Woolsey, *Cerebr. Cortex* **1**, 308 (1991); A. Agmon, L. T. Yang, D. K. O'Dowd, E. G. Jones, *J. Neurosci.* **13**, 5365 (1993).
7. R. S. Erzurumlu and S. Jhaveri, *Dev. Brain Res.* **56**, 229 (1990); M. E. Blue, R. S. Erzurumlu, S. Jhaveri, *Cerebr. Cortex* **1**, 380 (1991); S. Jhaveri, R. S. Erzurumlu, K. Crossin, *Proc. Natl. Acad. Sci. U.S.A.* **88**, 4489 (1991); B. L. Schlaggar and D. D. M. O'Leary, *J. Comp. Neurol.* **346**, 90 (1994).
8. S. M. Catalano, R. T. Robertson, H. P. Killackey, *Proc. Natl. Acad. Sci. U.S.A.* **92**, 2549 (1995); K. F. Jensen and H. P. Killackey, *J. Neurosci.* **7**, 3544 (1987).
9. H. Van der Loos, E. Welker, J. Dörfel, G. Rumo, *J. Hered.* **77**, 66 (1986).
10. W. F. Dietrich *et al.*, *Nature Genet.* **7**, 220 (1994).
11. G. R. Belford and H. P. Killackey, *J. Comp. Neurol.* **183**, 305 (1979); P. M. Ma, *ibid.* **309**, 161 (1991).
12. H. Van der Loos, *Neurosci. Lett.* **2**, 1 (1976).
13. D. Durham and T. A. Woolsey, *J. Comp. Neurol.* **223**, 424 (1984).
14. O. Cases *et al.*, *Science* **268**, 1763 (1995).
15. Experimental procedures were approved by the Office Vétérinaire Cantonal (Lausanne), in accordance with Swiss laws. Tracers were injected in adult mice that were anesthetized with Nembutal (60 mg of sodium pentobarbital per kilogram of body mass, intraperitoneal) and placed in a stereotaxic frame. Biotinylated dextran (5% in water) was iontophoretically injected (2 μ A of positive current, 7 s on and 7 s off for 15 min) through a glass pipette (diameter, 20 μ m). Biocytin (2% in 1 M potassium

Howard Hughes Medical Institute, Neurobiology Division, Department of Molecular and Cell Biology, 519 Life Sciences Addition, University of California, Berkeley, CA 94720, USA.

*To whom correspondence should be addressed.